Exact Analytical Evaluation of Second-Order PMD Impact on the Outage Probability for a Compensated System

Enrico Forestieri, *Fellow, IEEE,* and Giancarlo Prati, *Member, IEEE*

***Abstract*—An exact analytical method for evaluating the outage probability due to second-order polarization mode dispersion in a system with first-order compensation is presented. In an uncompensated system the outage is mainly due to the mean differential group delay, whereas higher order effects have low impact. It is shown that in a compensated system all orders contribute to the outage probability, whereas accounting for exact second-order only gives a slight overestimate. Approximate second-order models leaving residual higher order effects may lead to very different outage probabilities.**

***Index Terms*—Communication system performance, optical equalizers, optical fiber communication, optical fiber polarization, polarization mode dispersion (PMD).**

I. Introduction

POLARIZATION-MODE dispersion (PMD) causes pulse distortion and broadening and is an important source of limitation for the performance of high bit rate optical systems because of the arising intersymbol interference (ISI). In the first-order approximation, its effect is simply a differential group delay (DGD) $\Delta\tau$ of the pulse components travelling on the two orthogonal polarization states known as principal states (PSPs) [1]. The DGD $\Delta\tau$ is equal to the modulus of the PMD vector $\vec{\Omega}$, which is assumed to be independent of frequency over the signal bandwidth.

When $\vec{\Omega}$ has a nonnegligible dependence on frequency, higher order distortions take place. We point out that we use the Foschini and Poole interpretation of higher order PMD [2]. Even if alternative definitions exist [3], [4], a complete statistical characterization is currently available only for the dispersion vector and its derivative, so outage probabilities can be analytically evaluated only through their joint statistics, making Foschini and Poole's the natural interpretation of higher order PMD. In this second-order approximation, the dispersion vector is taken as linearly varying with frequency $\vec{\Omega} = \vec{\Omega}_0 + \vec{\Omega}_\omega(\omega - \omega_0), \vec{\Omega}_\omega$ being the derivative of $\vec{\Omega}$ with respect to ω evaluated at the carrier angular frequency ω_0. This frequency dependence is known to produce polarization dependent chromatic dispersion (PCD), through the component of $\vec{\Omega}_\omega$ parallel to $\vec{\Omega}_0$, and signal depolarization, through the component of $\vec{\Omega}_\omega$ orthogonal to $\vec{\Omega}_0$.

Manuscript received April 30, 2003; revised January 17, 2004. This work was supported by Marconi Communications and by MUIR under the PRIN project "OTDM."

The authors are with Scuola Superiore Sant'Anna di Studi Universitari e Perfezionamento, Pisa, Italy, and also with the Photonic Networks National Laboratory, CNIT, Pisa, Italy (e-mail: forestieri@sssup.it).

Digital Object Identifier 10.1109/JLT.2004.825361

To the authors' knowledge, there is only one work [5] on the theoretical outage probability evaluation in the presence of first- and second-order PMD, but using approximate second-order statistics, and a Gaussian assumption on the noise after photodetection. An analytical evaluation of the impact of first- and second-order PMD on a preamplified direct detection system using exact second-order statistics, evaluated as in [6], is presented here, confirming that higher order PMD impairments are masked in an uncompensated system [7], [8]. Indeed, in this case, the various analytical second-order approximations for the fiber Jones matrix taken into account [9]–[11] turn out to be almost equivalent in terms of resulting outage probability for the uncompensated system, but produce significant differences when a first order compensator is introduced in the system. As also observed in [3], it is rumored that when second-order PMD becomes important, then all other higher order terms become important too. The fiber Jones matrix model in [11] is an exact second-order model in the sense that second and higher order derivatives of its PMD vector vanish. By comparing the results from this model with those from simulations accounting for all PMD orders, we can investigate this aspect and also state the validity of the other second-order models when averaging is done through the joint statistics of the first- and second-order PMD vectors.

The paper is organized as follows. In Section II the theory of first- and second-order PMD is briefly reviewed and analytical formulas for the outage probability evaluation are presented for both the uncompensated and compensated cases. Section III deals with uncompensated systems, giving an accurate closed form approximation for the outage probability in the first-order case and showing that higher orders have no impact. Finally, in Section IV the case of exact first-order compensation is analyzed and the impact of second and residual higher PMD orders established by evaluating the outage probability and comparing the results when using various approximations of the second-order fiber Jones matrix.

II. Theoretical Model

The uncompensated system model and its lowpass equivalent are shown in Fig. 1(a) and (b), respectively, where double arrows denote optical signals. In Fig. 1(b) $\hat{x}(t) = x(t)\hat{e}_{\rm in}$, where $\hat{e}_{\rm in}$ is the input polarization state Jones vector and $x(t)$ is the lowpass equivalent of the transmitted bandpass signal $x_{\rm bp}(t) = \Re{\rm e}\{x(t)e^{j\omega_0 t}\}$; $\mathbf{F}(\omega)$ is the fiber Jones

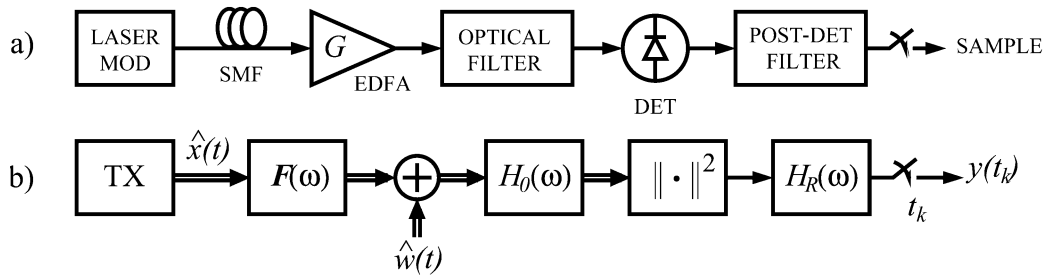

Fig. 1. (a) System model. (b) Corresponding lowpass equivalent.

matrix[1] ; $\hat{w}(t) = [w_1(t), w_2(t)]^T$, where $w_1(t)$ and $w_2(t)$ are independent complex additive white Gaussian noises (AWGN), accounting for the amplified spontaneous emission (ASE) noise, each with twosided power spectral density $N_0 = n_{\rm sp}(G-1)h\nu/G \simeq n_{\rm sp}h\nu, n_{\rm sp} \geq 1$ being the spontaneous emission parameter, $G \gg 1$ being the fiber amplifier gain and $h\nu$ the photon energy; $H_0(\omega)$ and $H_R(\omega)$ are the (lowpass equivalent) transfer functions of the optical and postdetection filters, respectively. It is assumed that the preamplifier has a high-gain G such that the ASE noise dominates over the thermal and shot noises.

Without loss of generality, we assume that the carrier polarization state remains unchanged, so that the fiber Jones matrix is taken as $\mathbf{F}(\omega) = \mathbf{R}\mathbf{U}(\omega)\mathbf{R}^{-1}$, where $\mathbf{U}(\omega)$ is one of the second-order approximations in [9]–[11], all referred to a reference frame in which, at the carrier frequency, their PMD vector is aligned with the S_1 axis in the Stokes space and such that $\mathbf{U}(0) = \mathbf{I}$. The matrix $\mathbf{U}(\omega)$ is then a generalized Jones matrix. All the second-order approximations for the fiber Jones matrix $\mathbf{U}(\omega)$ depend on three parameters evaluated at the carrier frequency, i.e., the DGD $\Delta\tau$, the DGD derivative with respect to angular frequency $\Delta\tau_\omega$, and the PMD vector rotation rate q_ω [12].

As the PMD versor $\vec{q} = \vec{\Omega}_0/|\vec{\Omega}_0|$, which we can assume to be coincident with the fast PSP at the carrier frequency, is uniformly distributed over the Poincaré sphere, $\mathbf{R}$ turns out to be a random rotation matrix, independent of frequency, and representing a change of basis polarization states. Its effect is to rotate the PMD vector such as to realize a uniformly distributed signal power splitting between the PSP's at the carrier frequency. The explicit expression for $\mathbf{R}$ is

$$\mathbf{R} = \begin{pmatrix} r_1 & -r_2^* \\ r_2 & r_1^* \end{pmatrix} \tag{1}$$

where

$$\begin{aligned} r_1 &= \cos\theta\cos\varepsilon - j\sin\theta\sin\varepsilon \\ r_2 &= \sin\theta\cos\varepsilon + j\cos\theta\sin\varepsilon \end{aligned} \tag{2}$$

and θ, ε are independent random variables, representing the fast PSP azimuth and ellipticity angle, respectively, with probability density functions

$$p_\theta(x) = \begin{cases} \frac{1}{\pi}, & -\frac{\pi}{2} \leq x \leq \frac{\pi}{2} \\ 0, & \text{otherwise} \end{cases} \tag{3}$$

$$p_\varepsilon(x) = \begin{cases} \cos 2x, & -\frac{\pi}{4} \leq x \leq \frac{\pi}{4} \\ 0, & \text{otherwise} \end{cases}. \tag{4}$$

[1]We use boldface symbols to denote matrices, a cap for Jones vectors and an arrow for Stokes vectors.

Please note that it is the premultiplication by $\mathbf{R}$ that causes the PMD vector rotation, i.e., the matrix $\mathbf{R}\mathbf{U}(\omega)$ has the same dispersion vector of $\mathbf{F}(\omega)$, which, at the carrier frequency, is $\vec{\Omega}_0 = \Delta\tau\vec{q}$, where

$$\vec{q} = [\cos 2\theta\cos 2\varepsilon, \sin 2\theta\cos 2\varepsilon, \sin 2\varepsilon]^T \tag{5}$$

whereas the matrix $\mathbf{U}(\omega)\mathbf{R}^{-1}$ would have the same dispersion vector of $\mathbf{U}(\omega)$, namely $\Delta\tau[1,0,0]^T$. Also notice that the columns of $\mathbf{R}$ are the PSPs at the carrier frequency *only*, and that they are uniformly distributed over the Poincaré sphere, too.

A. First-Order PMD

In the first-order approximation $\vec{\Omega} = \vec{\Omega}_0$, the matrix $\mathbf{U}$ is diagonal

$$\mathbf{U}(\omega) = \begin{pmatrix} e^{+j\omega\Delta\tau/2} & 0 \\ 0 & e^{-j\omega\Delta\tau/2} \end{pmatrix} \tag{6}$$

and the photodetected signal has a very simple expression, as shown in the following. Letting $Y(\omega) = H_0(\omega)X(\omega)$ and $\hat{e}_{\rm in} = (e_1, e_2)^T$, where

$$\begin{aligned} e_1 &= \cos\theta_s\cos\varepsilon_s - j\sin\theta_s\sin\varepsilon_s \\ e_2 &= \sin\theta_s\cos\varepsilon_s + j\cos\theta_s\sin\varepsilon_s \end{aligned} \tag{7}$$

θ_s and ε_s being the signal polarization state azimuth and ellipticity angle, respectively, at the optical filter output the Jones vector of the electric field is

$$\begin{aligned} \hat{E}_o(\omega) &= \mathbf{R}\mathbf{U}(\omega)\mathbf{R}^{-1}Y(\omega)\hat{e}_{\rm in} \\ &= \mathbf{R}\hat{E}(\omega) \end{aligned} \tag{8}$$

where

$$\hat{E}(\omega) = Y(\omega)\mathbf{U}(\omega)\mathbf{R}^{-1}\hat{e}_{\rm in}. \tag{9}$$

Denoting by 2φ the angle between the fast PSP $\vec{q}$ in (5) and the signal polarization state in Stokes space

$$\vec{e}_{\rm in} = [\cos 2\theta_s\cos 2\varepsilon_s, \sin 2\theta_s\cos 2\varepsilon_s, \sin 2\varepsilon_s]^T \tag{10}$$

we have that $\vec{q}\cdot\vec{e}_{\rm in} = \cos 2\varphi$, where

$$\begin{aligned} \cos 2\varphi = &\cos 2\theta\cos 2\epsilon\cos 2\theta_s\cos 2\epsilon_s \\ &+ \sin 2\theta\cos 2\epsilon\sin 2\theta_s\cos 2\epsilon_s \\ &+ \sin 2\epsilon\sin 2\epsilon_s. \end{aligned} \tag{11}$$

Letting $y(t) = \mathcal{F}^{-1}\{Y(\omega)\}, \hat{e}(t) = \mathcal{F}^{-1}\{\hat{E}(\omega)\}$ and $\hat{e}_o(t) = \mathbf{R}\hat{e}(t)$, where $\mathcal{F}^{-1}$ means Fourier antitransformation,

as $\mathbf{R}^{T*}\mathbf{R} = \mathbf{R}^{-1}\mathbf{R} = \mathbf{I}$, the photodetected signal before postdetection filtering is given by

$$\begin{aligned} s'_{\mathrm{PMD}}(t) &= |\hat{e}_o(t)|^2 \\ &= \hat{e}(t)^{T*}\mathbf{R}^{T*}\mathbf{R}\hat{e}(t) \\ &= |\hat{e}(t)|^2 \\ &= c_1|y(t+\Delta\tau/2)|^2 + c_2|y(t-\Delta\tau/2)|^2 \end{aligned} \quad (12)$$

and taking into account (2), (7), and (11), a simple calculation shows that

$$\begin{aligned} c_1 &= \frac{1}{2}(1+\cos 2\varphi) = \cos^2\varphi \\ c_2 &= \frac{1}{2}(1-\cos 2\varphi) = \sin^2\varphi. \end{aligned}$$

Hence, after postdetection filtering

$$s_{\mathrm{PMD}}(t) = \gamma s(t+\Delta\tau/2) + (1-\gamma)s(t-\Delta\tau/2) \quad (13)$$

where $s(t) = |y(t)|^2 \otimes h_R(t)$ is the signal in the absence of PMD, $h_R(t)$ being the postdetection filter impulse response and $\otimes$ denoting convolution, whereas $\gamma = \cos^2\varphi$ is the signal power splitting ratio between the PSPs. From (13), it can be seen that in the first-order approximation the photodetected signal depends only upon the DGD $\Delta\tau$ and the power splitting γ and is independent of the PMD vector orientation (given γ). This is no longer true for a second-order approximation where, other than the (further distorted) replicas in (13), other terms arise, somewhat complicating the expression for the photodetected signal. In the next section, we will give an expression for the output sample suitable for calculation, taking also into account the ASE noise.

B. Second-Order PMD

As long as an optical PMD compensator performs linearly with respect to the electrical field and can be modeled by a unitary Jones matrix, the compensated and uncompensated cases can be treated unitedly, as explained in the following for the theoretical example case of exact first-order compensation. So, let us assume to have a PMD compensator that perfectly compensate for first-order PMD. This goal can be achieved by inserting after the optical filter a polarization controller which is able to rotate the fiber PMD vector such that, at the carrier frequency, it is antiparallel to that of a retarded plate whose adjustable retardation is made equal to $\Delta\tau$. As the polarization controller and the retarded plate are characterized by unitary Jones matrices, they leave unchanged the ASE noise statistics, so we could have inserted them right at the fiber output with the same effect. This means that we can simply substitute the Jones matrix $\mathbf{F}(\omega)$ in Fig. 1(b) with $\mathbf{F}_c(\omega) = \mathbf{D}(\omega)\mathbf{R}^{-1}\mathbf{F}(\omega) = \mathbf{D}(\omega)\mathbf{U}(\omega)\mathbf{R}^{-1}$, where

$$\mathbf{D}(\omega) = \begin{pmatrix} \mathrm{e}^{-j\Delta\tau\omega/2} & 0 \\ 0 & \mathrm{e}^{+j\Delta\tau\omega/2} \end{pmatrix} \quad (14)$$

is the Jones matrix of the retarded plate whose fast and slow axes are exchanged with respect to those of $\mathbf{U}(\omega)$.

By extending the analysis in [13] to the present case, as shown in Appendix A, and denoting by T the bit time, the sample $y(t_k)$ corresponding to a periodic N-bit pattern can be written as

$$y(t_k) = d_k + r_k \quad (15)$$

where

$$d_k = \sum_{\ell=-2L}^{2L} (c_{1,\ell} + c_{2,\ell}) H_R\left(\frac{\ell}{NT}\right) e^{j2\pi\ell t_k/NT} \quad (16)$$

is the signal, whereas

$$\begin{aligned} r_k = 2\sum_{i=1}^{2M+1} \Re\mathrm{e}[z_{1,i}b^*_{1,i} + z_{2,i}b^*_{2,i}] \\ + \sum_{i=1}^{2M+1} \lambda_i(|z_{1,i}|^2 + |z_{2,i}|^2) \end{aligned} \quad (17)$$

is the noise due to signal-ASE and ASE-ASE beat, respectively, the subscripts 1 and 2 referring to the two reference orthogonal polarizations. We defer to Appendix A and [13] the explanation of the parameters appearing in (16) and (17).

At the carrier frequency, denoting by 2φ the angle between the fast PSP (assumed to have the same direction of $\vec{\Omega}_0$) and the signal polarization state in Stokes space (taken, without loss of generality, aligned along the S_2 axis), the signal power splitting ratio γ between the two PSPs may be written as[2] $\gamma = \cos^2\varphi = (1+\sin 2\theta\cos 2\varepsilon)/2$. Hence, to make a link with the first-order PMD case, we can equivalently describe the orientation of $\vec{\Omega}_0$ through the power splitting ratio γ, which can be shown to be uniformly distributed between 0 and 1

$$p_\gamma(x) = \begin{cases} 1, & 0 \le x \le 1 \\ 0, & \text{otherwise} \end{cases} \quad (18)$$

and the fast PSP ellipticity angle ε, whose probability density function (pdf), conditional upon γ, can be shown to be

$$p_\varepsilon(x\,|\,\gamma) = \begin{cases} \frac{\cos 2x}{\sin 2\varepsilon_\gamma}, & |x| \le \varepsilon_\gamma \\ 0, & \text{otherwise} \end{cases} \qquad \varepsilon_\gamma \triangleq \frac{1}{2}\arccos(|2\gamma-1|). \quad (19)$$

Being the decision threshold V and letting $\xi_k = V - d_k$, the conditional average probability of error $\mathcal{E}$, given a N-bit information sequence $\{a_n\}$, can be expressed as

$$\begin{aligned} P(\mathcal{E}\,|\,\Delta\tau, \Delta\tau_\omega, q_\omega, \gamma, \varepsilon) \\ = \frac{1}{N}\sum_{k=0}^{N-1} P(\mathcal{E}_k\,|\,\{a_n\}, \Delta\tau, \Delta\tau_\omega, q_\omega, \gamma, \varepsilon) \end{aligned} \quad (20)$$

where

$$\begin{aligned} P(\mathcal{E}_k\,|\,\{a_n\}, \Delta\tau, \Delta\tau_\omega, q_\omega, \gamma, \varepsilon) \\ = \begin{cases} P\{y(t_k) < V\} = P\{r_k < \xi_k\}, & \text{if } a_k = 1 \\ P\{y(t_k) > V\} = P\{r_k > \xi_k\}, & \text{if } a_k = 0 \end{cases} \end{aligned} \quad (21)$$

and, for simplicity, the conditioning on the PMD parameters has been omitted on the right-end side term. The probabilities $P\{r_k \gtrless \xi_k\}$ in (21) may be evaluated with high accuracy

[2]For a generic signal polarization state it would be $\gamma = [1 + \cos(2\theta - 2\theta_s)\cos 2\epsilon\cos 2\epsilon_s + \sin 2\epsilon\sin 2\epsilon_s]/2$, where θ_s and ϵ_s are the signal polarization state azimuth and ellipticity angle, respectively.

by using the saddle point approximation [13], requiring only knowledge of the noise sample r_k conditional moment generating function

$$\Psi_{r_k|\vec{\Omega}}(s) = \prod_{i=1}^{2M+1} \frac{\exp\left(\frac{\alpha_i \beta_i s^2}{1-\beta_i s}\right)}{(1-\beta_i s)^2} \tag{22}$$

where (see Appendix A) $\alpha_i = (|b_{1,i}|^2 + |b_{2,i}|^2)/\lambda_i$ and $\beta_i = 2\lambda_i \sigma^2$, the parameter σ^2 being the variance of the real and imaginary parts of the noise components $z_{1,i}$ and $z_{2,i}$ [13].

Defining the outage probability $P(\mathcal{O})$ as the probability that the bit error rate (BER) exceeds 10^{-12} given 3-dB sensitivity penalty with respect to the case of PMD absence, and averaging out second-order effects, the conditional (upon $\vec{\Omega}_0$) outage probability is

$$P(\mathcal{O} \,|\, \Delta\tau, \gamma, \varepsilon) = \iint_{\Delta\tau_\omega, q_\omega} u[P(\mathcal{E} \,|\, \Delta\tau, \Delta\tau_\omega, q_\omega, \gamma, \varepsilon) - 10^{-12}] \times p_{\Delta\tau_\omega, q_\omega}(\Delta\tau_\omega, q_\omega \,|\, \Delta\tau) d\Delta\tau_\omega dq_\omega \tag{23}$$

where $u(x)$ is the unit step function. The unconditional outage probability may then be evaluated as

$$P(\mathcal{O}) = \iiint_{\Delta\tau, \gamma, \varepsilon} P(\mathcal{O} \,|\, \Delta\tau, \gamma, \varepsilon) p_{\Delta\tau}(\Delta\tau) p_\gamma(\gamma) \times p_\varepsilon(\varepsilon \,|\, \gamma) d\varepsilon d\gamma d\Delta\tau. \tag{24}$$

The purpose of this two-step evaluation for the outage probability is that by averaging out second-order effects, as in (23), we can judge about their impact. As regards the averaging in (24), the pdfs $p_\gamma(\gamma)$ and $p_\varepsilon(\varepsilon \,|\, \gamma)$ are as in (18) and (19), respectively, whereas the pdf $p_{\Delta\tau}(\Delta\tau)$ is the well-known Maxwellian [14]

$$p_{\Delta\tau}(x) = \sqrt{\frac{2}{\pi}} \frac{x^2}{\mu^3} e^{-\frac{x^2}{2\mu^2}} u(x) \tag{25}$$

where $\mu = \sqrt{\pi/8}\langle\Delta\tau\rangle$ is the standard deviation of each component of the dispersion vector $\vec{\Omega}_0$, $\langle\Delta\tau\rangle$ being the mean DGD value. Notice that in the first-order approximation the conditional outage probability in (23) is simply equal to 0 or 1 as in this case $P(\mathcal{O} \,|\, \Delta\tau, \gamma, \varepsilon) = P(\mathcal{O} \,|\, \Delta\tau, \gamma) = u[P(\mathcal{E} \,|\, \Delta\tau, \gamma) - 10^{-12}]$ and in (24) the ellipticity angle pdf $p_\varepsilon(\varepsilon \,|\, \gamma)$ directly integrates to 1 as the conditional outage probability does not depend on ε (given γ). For the second-order approximation, the joint pdf $p_{\Delta\tau_\omega, q_\omega}(x, y \,|\, \Delta\tau)$, needed to perform the averaging in (23), may be evaluated as follows. Denoting by $\tilde{\Omega}_0 \triangleq \vec{\Omega}_0/\mu$ and $\tilde{\Omega}_\omega \triangleq \vec{\Omega}_\omega/\mu^2$ the PMD vector and its derivative normalized to μ and μ^2, respectively, and by $\Omega_{\omega\|} = \Delta\tau_\omega/\mu^2$ and $\Omega_{\omega\perp} = \Delta\tau q_\omega/\mu^2$ the parallel and (modulus of) the orthogonal components of $\tilde{\Omega}_\omega$ with respect to $\tilde{\Omega}_0$, we have that

$$p_{\Delta\tau_\omega, q_\omega}(x, y \,|\, \Delta\tau) = \frac{\Delta\tau}{\mu^4} p_{\Omega_{\omega\|}, \Omega_{\omega\perp}}\left(\frac{x}{\mu^2}, \frac{\Delta\tau y}{\mu^2}\middle| \Delta\tau\right) \tag{26}$$

where $p_{\Omega_{\omega\|}, \Omega_{\omega\perp}}(x, y \,|\, \Delta\tau)$ can be efficiently evaluated as explained in [6].

III. Uncompensated Systems

In this section, we evaluate the outage probability due to first- and second-order PMD in the case of uncompensated systems. The first-order case has been extensively treated in the literature [15]–[17], but we give here a short account to present an upper bound closed form expression for the outage probability which we will relate to the approximation given in [16] to show how its range of validity can be extended. In this and the following sections a Gaussian shaped optical filter and a 5th order Bessel postdetection filter with 3-dB bandwidths equal to $1.875R_b$ and $0.75R_b$, respectively, were assumed for the calculations ($R_b = 1/T$ is the bit rate). The signal format is NRZ and the electric field pulse shape is that of a rectangular pulse filtered by a Gaussian filter with 3-dB bandwidth $0.8R_b$. A 2^5-bit de Bruijn sequence was chosen such that to account for the ISI due to four adjacent bits [13].

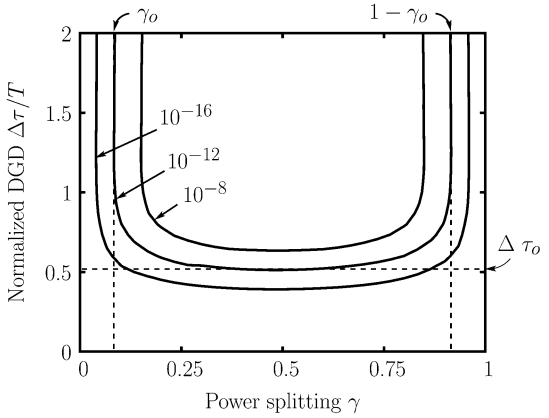

Fig. 2. BER contour plots for 3-dB sensitivity penalty.

A. First-Order PMD

In this case, (24) becomes

$$P(\mathcal{O}) = \iint_R p_{\Delta\tau}(\Delta\tau) p_\gamma(\gamma) d\gamma d\Delta\tau \tag{27}$$

where R is the region of the $\gamma, \Delta\tau$ plane where $\mathrm{BER} > 10^{-12}$. In this plane, the iso-BER curves have a typical U-shape, as shown in Fig. 2, suggesting a simple closed form upper bound for $P(\mathcal{O})$. Indeed, we see that there is a value γ_o for the power splitting such that for $\gamma < \gamma_o$, or $\gamma > 1-\gamma_o$, the BER is always less than 10^{-12} whatever the DGD $\Delta\tau$, and, similarly, there is a value $\Delta\tau_o$ for the DGD such that, for $\Delta\tau < \Delta\tau_o, \mathrm{BER} < 10^{-12}$ whatever the value of γ. So, integrating $p_{\Delta\tau}(\Delta\tau) p_\gamma(\gamma)$ over the rectangular region $\{\gamma_o \le \gamma \le 1-\gamma_o, \Delta\tau \ge \Delta\tau_o\}$, we obtain the upper bound

$$\begin{aligned} P(\mathcal{O}) &< \left(\frac{1}{2} - \gamma_o\right) \left\{ 2\,\mathrm{erfc}\left(\frac{2\Delta\tau_o}{\sqrt{\pi}\langle\Delta\tau\rangle}\right) + \frac{8\Delta\tau_o}{\pi\langle\Delta\tau\rangle} \exp\left[-\frac{4}{\pi}\left(\frac{\Delta\tau_o}{\langle\Delta\tau\rangle}\right)^2\right] \right\} \\ &< \left(\frac{1}{2} - \gamma_o\right) \left(\frac{\langle\Delta\tau\rangle}{\Delta\tau_o} + \frac{8\Delta\tau_o}{\pi\langle\Delta\tau\rangle}\right) \times \exp\left[-\frac{4}{\pi}\left(\frac{\Delta\tau_o}{\langle\Delta\tau\rangle}\right)^2\right] \end{aligned} \tag{28}$$

where we used the inequality $\mathrm{erfc}(x) < \exp(-x^2)/(x\sqrt{\pi})$. Notice that the U-shaped iso-BER curves are symmetric around $\gamma = 0.5$ only if the postdetection filter impulse response is symmetric, but usually their asymmetry is not noticeable.

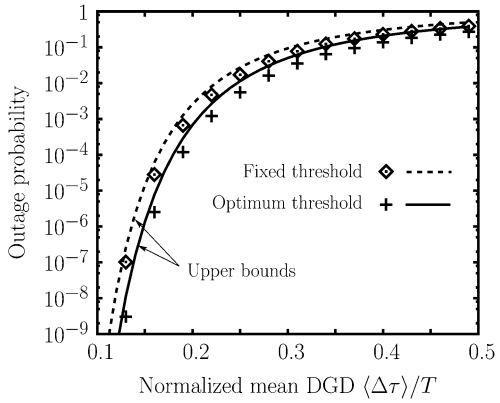

Fig. 3. Outage probability due to first-order PMD for 3-dB sensitivity penalty.

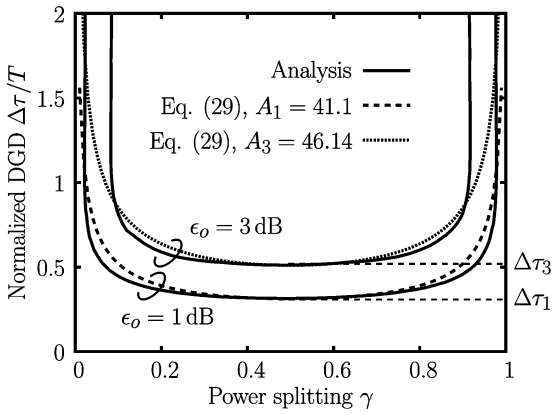

Fig. 4. Penalty contour plots for BER $= 10^{-12}$.

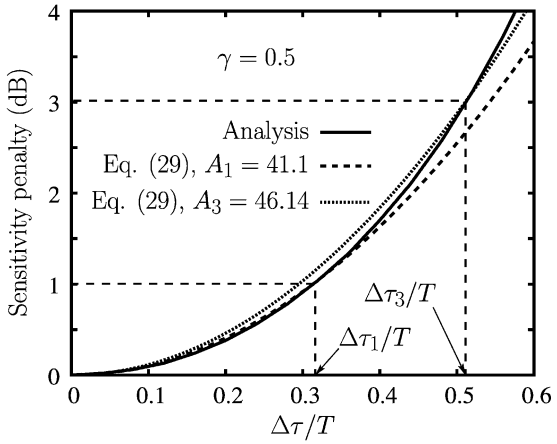

Fig. 5. Sensitivity penalty versus normalized DGD.

The outage probability evaluated as in (27) and the upper bound (28) are shown in Fig. 3 for the cases of optimum and fixed detection threshold. In the optimum threshold case, the BER was evaluated by optimizing the threshold for each PMD realization, whereas in the fixed threshold case the threshold was set to its optimum value in the absence of PMD and then was held fixed. This last case is more realistic as in a real receiver the threshold is usually set once for all and not changed afterwards. It can be seen that this could lead to outage probabilities larger than an order of magnitude. We point out that this analysis is not possible by using one of the various Gaussian approximations in the literature, as they are accurate only when optimizing the threshold, which, however, is not the real optimum threshold [18]. Anyhow, we verified that using a fixed threshold only slightly larger than the optimum one in the absence of PMD, leads to the same outage probability obtained by optimizing the threshold for each PMD outcome, thus justifying the use of Gaussian approximations in the PMD case, too.

Sometimes the outage probability is defined as the probability that the sensitivity penalty ϵ in dB exceeds a given value ϵ_o to maintain a given BER P_e [16]. It is easy to show that this definition is equivalent to the one we use, i.e., the probability that the BER exceeds P_e given the sensitivity penalty ϵ_o. The advantage of our definition is that it is easier to generate the iso-BER curves of Fig. 2 rather than the corresponding iso-penalty curves. The advantage of the other definition is that an approximate expression for ϵ, expressed in dB, is available [16]

$$\epsilon \simeq A\left(\frac{\Delta\tau}{T}\right)^2 \gamma(1-\gamma) \tag{29}$$

where A depends on the pulse shape and receiver characteristics, and thus the outage probability can be evaluated in closed form. Indeed, from (29) and taking into account (18) and (25), we have that the pdf of ϵ is [16]

$$p_\epsilon(x) \simeq \eta e^{-\eta x} u(x) \tag{30}$$

where

$$\eta = \frac{16}{A\pi\left(\langle\Delta\tau\rangle/T\right)^2} \tag{31}$$

and, thus

$$P(\mathcal{O}) = P(\epsilon \geq \epsilon_o) \simeq \int_{\epsilon_o}^{\infty} \eta e^{-\eta\epsilon} d\epsilon = e^{-\epsilon_o \eta}. \tag{32}$$

In [16], (32) was only used with $\epsilon_o = 1$ dB as (29) is valid only for small penalties. Despite this fact, we will now show that (32) can be also used for larger values of ϵ_o and that it is a very close approximation to $P(\mathcal{O})$ when parameter A is properly chosen. In Fig. 4 the analytically evaluated iso-penalty curves are drawn in solid lines, whereas dashed lines were obtained from (29) with $\epsilon_o = 1$ and 3 dB, respectively, and a proper choice for parameter A. Parameter A is usually chosen by a quadratic fit of the PMD penalty according to (29) for $\gamma = 0.5$ [17]. We make here a different choice and consider A as a function of ϵ_o, $A = A_{\epsilon_o}$, obtaining it from (29), by setting $\epsilon = \epsilon_o, \gamma = 0.5$ and $\Delta\tau = \Delta\tau_{\epsilon_o}$, as

$$A_{\epsilon_o} = \frac{4\epsilon_o}{(\Delta\tau_{\epsilon_o}/T)^2} \tag{33}$$

where $\Delta\tau_{\epsilon_o}$ can be acquired from the corresponding iso-penalty curve obtained by analysis, as illustrated in Fig. 4, or, simply, as the instantaneous DGD corresponding to $\epsilon = \epsilon_o$ for $\gamma = 0.5$, as illustrated in Fig. 5. Notice from this last figure that for $\epsilon_o = 1$ dB, this choice for $\Delta\tau_{\epsilon_o}$ gives a parameter A from (33) making (29) a quadratic fit to the PMD penalty. It turned out that $A_1 = 41.1$ and $A_3 = 46.14$, in this case, and using these values for parameter A in (31) the outage probability evaluated as in (32) is shown in Fig. 6 together with that evaluated through (27), where now R is the region of the $\gamma, \Delta\tau$ plane where $\epsilon > \epsilon_o$. Notice that the iso-penalty curve for $\epsilon_o = 3$ dB in Fig. 4 exactly

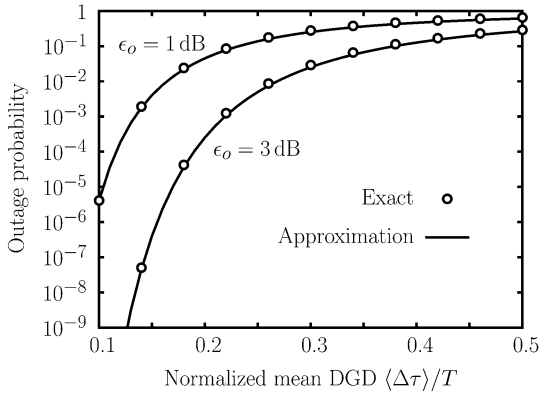

Fig. 6. Outage probability due to first-order PMD for 1- and 3-dB sensitivity penalty.

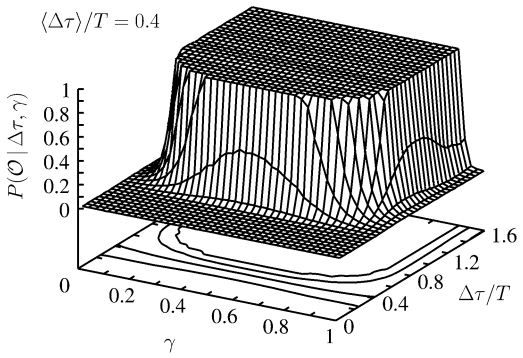

Fig. 7. Conditional outage probability due to first- and second-order PMD for 3-dB sensitivity penalty. The contours are at 10^{-5}, 10^{-3}, 10^{-1}, and 1.

corresponds to the $\mathrm{BER} = 10^{-12}$ curve in Fig. 2 and that, for our choice of parameter A and except for a multiplicative factor

$$P(\mathcal{O}) \simeq \exp\left[-\frac{4}{\pi}\left(\frac{\Delta\tau_{\epsilon_o}}{\langle\Delta\tau\rangle}\right)^2\right] \tag{34}$$

is practically equal to (28), $\Delta\tau_{\epsilon_o}$ playing the same role of $\Delta\tau_o$. Also, notice that (28) is an upper bound, whereas (34) is an approximation.

B. Second-Order PMD

In this case, $P(\mathcal{O}\,|\,\Delta\tau,\gamma,\varepsilon)$ is no longer equal to 0 or 1, and Fig. 7 shows the conditional probability $P(\mathcal{O}\,|\,\Delta\tau,\gamma)$, evaluated as in (23) and further averaged over the ellipticity angle ε, through $p_\varepsilon(\varepsilon\,|\,\gamma)$, for a mean DGD equal to 40% of bit time when using the model in [10] for $\mathbf{U}(\omega)$. We noticed that the dependence of $P(\mathcal{O}\,|\,\Delta\tau,\gamma,\varepsilon)$ on ε is not marked and this means that, for a given power splitting γ, the orientation of $\vec{\Omega}_0$ is not so important (remember that in the first-order case even the photodetected signal was independent of this orientation). As can be seen from Fig. 7, the conditional outage probability changes very rapidly from low values to 1 when the instantaneous DGD and power splitting approach the values enclosed in the region delimited by the 10^{-1} contour curve. For a first-order PMD we would have a similar region in which the conditional outage probability would be equal to 1 and outside of which it would be exactly equal to zero. Whatever the value of $\Delta\tau$ and γ, the conditional outage probability is not negligible, even when

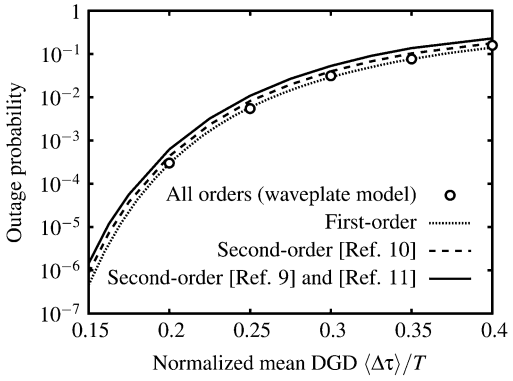

Fig. 8. Outage probability for 3-dB sensitivity penalty.

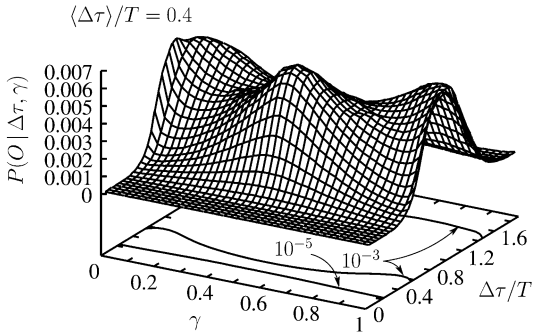

Fig. 9. Conditional outage probability due to second-order PMD for exact first-order compensation and 3-dB sensitivity penalty.

launching the signal with a polarization aligned with one of the PSPs at the carrier frequency, i.e., for $\gamma = 0$ or 1. However, the unconditional outage probability $P(\mathcal{O})$ is not affected by higher orders, as can be seen from Fig. 8, reporting $P(\mathcal{O})$ as a function of the mean DGD and showing that the models in [9]–[11] are practically equivalent, that in [10] being slightly more accurate. Fig. 8 also reports the outage probability computed by a Monte Carlo method by modeling the fiber through the random waveplate model with 100 sections. A sufficient number of fiber realizations was used such that the confidence interval is smaller than the circle used for representation. Notice that whereas the second-order analytical models for $\mathbf{U}(\omega)$ give slightly larger outages, the first-order model is in excellent agreement with the random waveplate model. Our results agree with those reported in [19], where the same approximate joint pdf as that in [5] was used for averaging, further demonstrating that, when not compensating, higher PMD orders are not of concern. This can also be confirmed by comparing the curve for $\epsilon_o = 1$ dB in Fig. 6, accounting for first-order only PMD, with the curve for the OOK-NRZ case in [[20] Fig. 5(a)], accounting for all-order PMD.[3] For example, to have $P(\mathcal{O}) < 10^{-4}$, Fig. 6 prescribes $\langle\Delta\tau\rangle < 0.12T$, whereas from [[20] Fig. 5(a)] we have $\langle\Delta\tau\rangle < 0.14T$. Although from this comparison it may seem that first-order PMD overestimates the power penalty, this is not the case as our simulations for all-orders PMD exactly match those in Fig. 6. We think that the small difference between Figs. 6 and 5(a) in [20] is to be attributed to the fact that we use exact statistics for the post-detection noise and not Gaussian

[3]Please note that the x axis of Fig. 6 reports $\langle\Delta\tau\rangle/T$, whereas that of Fig. 5(a) in [20] reports $\sqrt{\langle\Delta\tau^2\rangle}/T$.

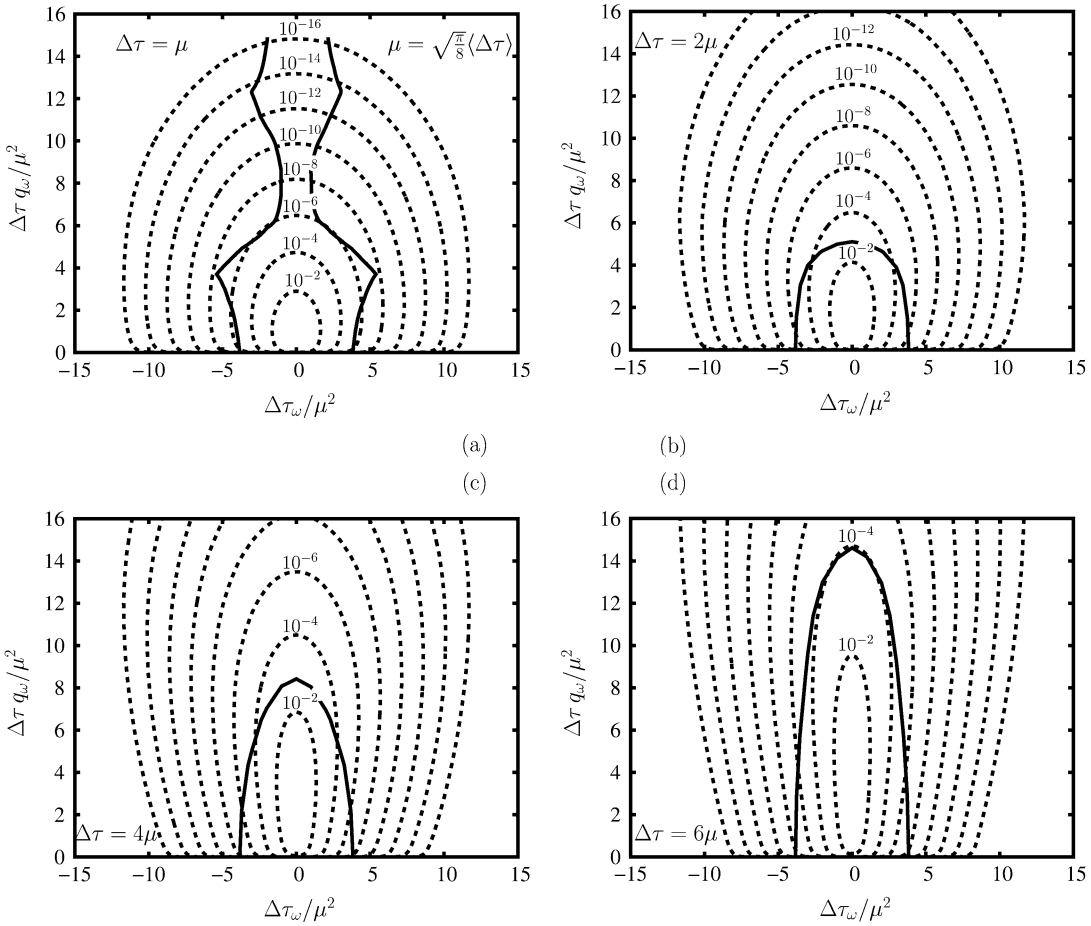

Fig. 10. Contour plot for BER $= 10^{-12}$ (solid) and for $p_{\Omega_{\omega||},\Omega_{\omega\perp}}(x, y \,|\, \Delta\tau)$ at $10^{-n}, n = 2, 4, 6, 8, 10, 12, 14, 16$. Power splitting $\gamma = 0.5$ and PSP ellipticity angle $\varepsilon = 0$.

approximations. However, we point out that if the outage probability is defined in a different manner, different conclusions may be drawn, as shown in [21].

IV. Exact First-Order Compensation

As explained in Section II-B, by using a polarization controller and a retarded plate with adjustable retardation, we can theoretically cancel the vector $\vec{\Omega}_0$ so that the performance is solely determined by higher PMD orders. All the models for the fiber Jones matrix in [9]–[11] agree on first- and second-order PMD, in the sense that they give the same dispersion vector $\vec{\Omega}_0$ and first-order derivative $\vec{\Omega}_\omega$, but whereas the model in [11] is an exact second-order model for which all higher order derivatives of $\vec{\Omega}$ vanish, the models in [9], [10] introduce higher orders. As seen in the previous section, in uncompensated systems the outage probability is due to first-order only, and indeed all theoretical models for $\mathbf{U}(\omega)$ turn out to be almost equivalent in this respect. When cancelling $\vec{\Omega}_0$, it is expected that this no more true.

Let us first see what is the effect of exact first-order compensation on the conditional outage probability $P(\mathcal{O} \,|\, \Delta\tau, \gamma)$. As the results are qualitatively almost the same, we consider in our examples the model in [10]. Fig. 9, to be compared with Fig. 7, reports $P(\mathcal{O} \,|\, \Delta\tau, \gamma)$ for the mean DGD $\langle\Delta\tau\rangle = 0.4T$ and it is evident that the conditional outage has not been changed for values of $\Delta\tau$ smaller than about $0.2T$, has been reduced by more than 2 orders of magnitude around $\Delta\tau = T$ and by more than three orders of magnitude for larger values of the DGD. The fact that for small DGD values $P(\mathcal{O} \,|\, \Delta\tau, \gamma)$ does not change should be expected as, for these values, the higher orders and not the DGD are the cause of outage, whereas, in part as guessed in [22], the impact of second-order PMD initially increases but then decreases for larger values of the instantaneous DGD. Taking now into consideration the impact of the $\vec{\Omega}_\omega$ components parallel and orthogonal to $\vec{\Omega}_0$, we report in Fig. 10 the iso-BER curve at 10^{-12} (solid) and contour plots of the joint pdf $p_{\Omega_{\omega||},\Omega_{\omega\perp}}(x, y \,|\, \Delta\tau)$ (dashed), where $\Omega_{\omega||} = \Delta\tau_\omega/\mu^2$ and $\Omega_{\omega\perp} = \Delta\tau q_\omega/\mu^2$ are the aforementioned components normalized to μ^2, for $\gamma = 0.5, \varepsilon = 0$ and various $\Delta\tau$ values. By integrating $p_{\Omega_{\omega||},\Omega_{\omega\perp}}(x, y \,|\, \Delta\tau)$ over the region outside the BER $= 10^{-12}$ curve we would obtain the conditional outage probability due to $\Omega_{\omega||}$ and $\Omega_{\omega\perp}$. Fig. 10 shows that for large DGD values the primary cause of outage is the orthogonal component $\Omega_{\omega\perp}$, whereas for small DGD values it is the parallel component $\Omega_{\omega||}$. In fact, for $\Delta\tau = \mu$, Fig. 10(a) tells us that if $\Omega_{\omega||} = 0$, i.e., if $\Delta\tau_\omega = 0$, no outage would occur. However, we point out that this result comes from the model in [10], as the other models in [9], [11], for small DGD values, produce iso-BER curves similar to the ones in Fig. 10(b), (c), and (d). However, when evaluating the unconditional outage, we see that the model in [10] is the most accurate, giving outages nearly equal to those obtained by the random waveplate model and

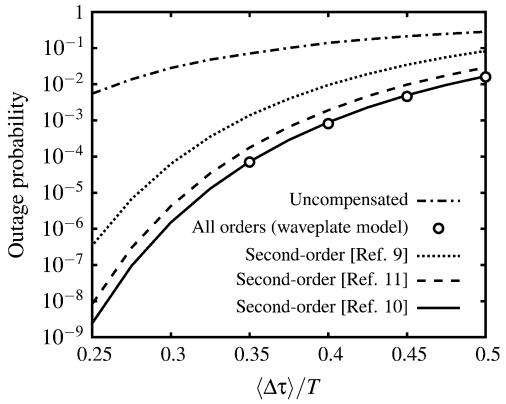

Fig. 11. Outage probability for exact first-order compensation and 3-dB sensitivity penalty.

Monte Carlo estimation, as shown in Fig. 11, where, for comparison, the outage probability for the uncompensated system is also reported. As can be seen, the model in [9] overestimates the outage by even two orders of magnitude, whereas the exact second-order model in [11] by only a factor $2 \div 3$. From these results we infer that in compensated systems all PMD orders contribute in determining the performance and that the impact of higher than second orders is beneficial. As observed in [11], the model in [10] seemingly is not a so good second-order only approximation, and, indeed, we think that it is to be considered an approximation to all orders obtained with first- and second-order only parameters. This seems reasonable as the various orders are correlated [23],[24] and thus higher orders are also partly determined by lower orders. Thus, the higher orders introduced by the model in [10] are, in this sense, appropriate. On the contrary, the model in [9] introduces inappropriate higher orders, leading to orders-of-magnitude outage probability overestimation.

V. Conclusion

An exact analytical evaluation of the impact of second-order PMD on a preamplified direct detection system using exact second-order statistics has been presented. The analytical tool allows to establish the impact of second-order PMD through conditional results not otherwise possible by Monte Carlo simulations, even, perhaps, by using importance sampling techniques, and in a very reasonable time. As an example, to obtain outage probabilities in the order of 10^{-4} with a sufficiently small confidence interval through simulation, a few days computing time are necessary using current high speed computers, whereas a few hours suffice by analysis for any outage values. However, simulation still remains a necessary tool to account for all PMD orders and comparison with results obtained by Monte Carlo methods shows that exact second-order only turns out to be slightly pessimistic, whereas attention must be paid in using approximate second-order models leaving residual higher order effects as this may lead to orders-of-magnitude outage overestimation.

Appendix A

In this appendix, we give an expression for the sample $y(t_k)$ in Fig. 1 by extending the results of [13, App. A]. The expression in [13] for the sample $y(t_k)$ was given by neglecting the ASE noise in the polarization orthogonal to the signal as no polarization dispersion was taken into account and thus it could be eliminated by a polarizer. Anyway, in the absence of PMD, even if accounted for, it would give a signal independent noise term in the output, i.e., only an ASE-ASE beat term which can be neglected with respect to the other noise terms (its impact would be maximum, and in the order of about 0.3 dB, in a back-to-back configuration only). Here, instead, we are in the presence of polarization mode dispersion and we must take into account both signal and noise components in the two reference orthogonal polarizations.

Denoting by $s_p(t)$ and $n_p(t), p = 1, 2$, the signal and noise components in the two orthogonal reference polarizations at the optical filter output, the signal $y(t)$ at the decision gate is given by

$$y(t) = [|s_1(t) + n_1(t)|^2 + |s_2(t) + n_2(t)|^2] \otimes h_R(t) \quad \text{(A.1)}$$

where, given a periodic N-bit pattern, each term $|s_p(t) + n_p(t)|^2, p = 1, 2$, is as [13, eq. (A.7)], and thus the output sample can be written as

$$y(t_k) = y_1(t_k) + y_2(t_k) \quad \text{(A.2)}$$

where each $y_p(t_k), p = 1, 2$, is as in [13, eq. (A.27)], for convenience rewritten here for polarization p as

$$y_p(t_k) = \sum_{i=1}^{2M+1} \lambda_i \left| z_{p,i} + \frac{b_{p,i}}{\lambda_i} \right|^2 + \sum_{\ell=-2L}^{2L} c_{p,\ell} H_R\left(\frac{\ell}{NT}\right) e^{j2\pi \ell t_k/NT} - \sum_{i=1}^{2M+1} \frac{|b_{p,i}|^2}{\lambda_i}. \quad \text{(A.3)}$$

Taking into account that

$$\sum_{i=1}^{2M+1} \lambda_i \left| z_{p,i} + \frac{b_{p,i}}{\lambda_i} \right|^2 = \sum_{i=1}^{2M+1} \lambda_i |z_{p,i}|^2 + 2 \sum_{i=1}^{2M+1} \Re\mathrm{e}[z_{p,i} b_{p,i}^*] + \sum_{i=1}^{2M+1} \frac{|b_{p,i}|^2}{\lambda_i^2}. \quad \text{(A.4)}$$

Equation (A.3) can also be written as

$$y_p(t_k) = \sum_{\ell=-2L}^{2L} c_{p,\ell} H_R\left(\frac{\ell}{NT}\right) e^{j2\pi \ell t_k/NT} + 2 \sum_{i=1}^{2M+1} \Re\mathrm{e}[z_{p,i} b_{p,i}^*] + \sum_{i=1}^{2M+1} \lambda_i z_{p,i}^2 \quad \text{(A.5)}$$

where, in the right-hand side, the first term is the signal whereas the second and third are the signal-ASE and ASE-ASE beat, respectively. All parameters appearing in (A.5) are as in [13], and in particular: i) $c_{1,\ell}, c_{2,\ell}$ are the coefficients of the Fourier series expansion of the squared modulus of the signal components on the two reference orthogonal polarizations; ii) $z_{1,i}, z_{2,i}$ are the components of the independent random Gaussian vectors $\mathbf{z}_1, \mathbf{z}_2$ with zero mean and covariance matrix $E\{\mathbf{z}_p^* \mathbf{z}_p^T\} = 2\sigma^2 \mathbf{I}$, $p = 1, 2$, where $\sigma^2 = N_0/(2T_0)$, T_0 being a time interval depending only upon the optical and postdetection filters [13]; iii) λ_i are the eigenvalues of the Hermitian matrix $\mathbf{A} = \mathbf{H}^{T*}\mathbf{Q}\mathbf{H} = \mathbf{W}\Lambda\mathbf{W}^{T*}$, where $\mathbf{Q}$ is the matrix with elements[4] $q_{ij} = H_R(j - i/T_0), i, j = 1, 2, \ldots, 2M + 1$, $\mathbf{H}$

[4]Please, note that [13] erroneously reports $q_{ij} = H_R((i - j)/T_0)$.

and Λ are diagonal matrices with elements $H_0(i-M-1/T_0)$ and λ_i, respectively, and $\mathbf{W}$ is the matrix of the normalized eigenvectors; iv) $b_{1,i}, b_{2,i}$ are the components of the vectors $\mathbf{b}_p = \mathbf{W}^{T*}\mathbf{H}^{T*}\mathbf{v}_p, p = 1, 2$, where the vectors $\mathbf{v}_p$ are as in [13, eq. (A.13)], but referred to the signal components on the two reference orthogonal polarizations.

REFERENCES

[1] C. D. Poole and R. E. Wagner, "Phenomenological approach to polarization dispersion in long single-mode fibers," *Electron. Lett.*, vol. 22, no. 19, pp. 1029–1030, 1986.

[2] G. J. Foschini and C. D. Poole, "Statistical theory of polarization dispersion in single mode fibers," *J. Lightwave Technol.*, vol. 9, pp. 1439–1456, Nov. 1991.

[3] H. Kogelnik, L. E. Nelson, and J. P. Gordon, "Emulation and inversion of polarization-mode dispersion," *J. Lightwave Technol.*, vol. 21, no. 2, pp. 482–495, Feb. 2003.

[4] A. Vannucci and A. Bononi, "Statistical characterization of the Jones matrix of long fibers affected by polarization mode dispersion (PMD)," *J. Lightwave Technol.*, vol. 20, pp. 811–821, May 2002.

[5] H. Bülow, "System outage probability due to first- and second-order PMD," *IEEE Photon. Technol. Lett.*, vol. 10, pp. 696–698, May 1998.

[6] E. Forestieri, "A fast and accurate method for evaluating joint second-order PMD statistics," *J. Lightwave Technol.*, vol. 21, pp. 2492–2952, Nov. 2003.

[7] L. M. Gleeson, E. S. R. Sikora, and M. J. O. Mahoney, "Experimental and numerical investigation into the penalties induced by second order polarization mode dispersion at 10 Gb/s," in *Proc. ECOC'97*, vol. 1, 1997, pp. 15–18.

[8] D. Penninckx and F. Bruyère, "Impact of the statistics of second-order polarization-mode dispersion on systems performance," in *Proc. OFC'98 Tech. Dig.*, 1998, Paper ThR2, pp. 340–342.

[9] A. Eyal, W. K. Marshall, M. Tur, and A. Yariv, "Representation of second-order polarization mode dispersion," *Electron. Lett.*, vol. 35, no. 19, pp. 1658–1659, 1999.

[10] H. Kogelnik, L. E. Nelson, J. P. Gordon, and R. M. Jopson, "Jones matrix for second-order polarization mode dispersion," *Opt. Lett.*, vol. 25, no. 1, pp. 19–21, 2000.

[11] E. Forestieri and L. Vincetti, "Exact evaluation of the Jones matrix of a fiber in the presence of polarization mode dispersion of any order," *J. Lightwave Technol.*, vol. 17, pp. 1898–1909, Dec. 2001.

[12] G. J. Foschini, R. M. Jopson, L. E. Nelson, and H. Kogelnik, "The statistics of PMD-induced chromatic fiber dispersion," *J. Lightwave Technol.*, vol. 17, pp. 1560–1565, Sept. 1999.

[13] E. Forestieri, "Evaluating the error probability in lightwave systems with chromatic dispersion, arbitrary pulse shape and pre- and post-detection filtering," *J. Lightwave Technol.*, vol. 18, pp. 1493–1503, Nov. 2000.

[14] G. J. Foschini, L. E. Nelson, R. M. Jopson, and H. Kogelnik, "Probability densities of second-order polarization mode dispersion including polarization dependent chromatic fiber dispersion," *IEEE Photon. Technol. Lett.*, vol. 12, pp. 293–295, Mar. 2000.

[15] C. D. Poole, R. W. Tkach, A. R. Chraplyvy, and D. A. Fishman, "Fading in lightwave systems due to polarization-mode dispersion," *IEEE Photon. Technol. Lett.*, vol. 3, pp. 68–70, Jan. 1991.

[16] C. D. Poole and J. Nagel, "Polarization effects in lightwave systems," in *Optical Fiber Telecommunications IIIA*, I. P. Kaminov and T. L. Koch, Eds. New York: Academic, 1997.

[17] P. J. Winzer, H. Kogelnik, C. H. Kim, H. Kim, R. M. Jopson, and L. E. Nelson, "Effect of receiver design on PMD outage for RZ and NRZ," in *Proc. OFC'02*, 2002, Paper TuI1, pp. 46–48.

[18] P. A. Humblet and M. Azizoğlu, "On the bit error rate of lightwave systems with optical amplifiers," *J. Lightwave Technol.*, vol. 9, pp. 1576–1582, Nov. 1991.

[19] A. Orlandini and L. Vincetti, "Comparison of the Jones matrix analytical models applied to optical system affected by high-order PMD," *J. Lightwave Technol.*, vol. 21, pp. 1456–1464, June 2003.

[20] C. Xie, L. Moller, H. Haunstein, and S. Hunsche, "Polarization mode dispersion induced impairments in different modulation format systems," in *Proc. OFC 2003*, Mar. 2003, Paper TuO1, pp. 258–259.

[21] A. O. Lima, I. T. Lima, T. Adali, and C. R. Menyuk, "Comparison of power penalties due to first- and all-order PMD distortions," presented at the ECOC'02, 2002, Paper 7.1.2.

[22] G. Shtengel, E. Ibragimov, M. Rivera, and S. Suh, "Statistical dependence between first and second-order pmd," presented at the OFC'01, 2001, MO-3.

[23] M. Karlsson and J. Brentel, "Autocorrelation function of the polarization-mode dispersion vector," *Opt. Lett.*, vol. 24, no. 14, pp. 939–941, 1999.

[24] M. Shtaif, A. Mecozzi, and J. A. Nagel, "Mean-square magnitude of all orders of polarization mode dispersion and the relation with the bandwidth of the principal states," *IEEE Photon. Technol. Lett.*, vol. 12, pp. 696–698, Jan. 2000.

Enrico Forestieri (S'91–M'92–F'03) was born in Milazzo, Italy, in 1960. He received the Dr.Ing. degree in electronics engineering from the University of Pisa, Pisa, Italy, in 1988.

From 1989 to 1991, he was a Postdoctoral Scholar at the University of Parma, Parma, Italy, working in optical communication systems. From 1991 to 2000, he was a Research Scientist and Faculty Member of the University of Parma. He is now an Associate Professor of Telecommunications at the Scuola Superiore S ant'Anna, Pisa, Italy. His research interests are in the area of digital communication theory and optical communication systems.

Giancarlo Prati (M'81) was born in Rome, Italy, in 1946. He received the Dr.Ing. degree in electronics engineering (*cum laude*) from the University of Pisa, Pisa, Italy, in 1972.

From 1975 to 1978, he was an Associate Professor of Electrical Engineering at the University of Pisa. From 1978 to 1979, he was on a NATO-supported Fellowship Leave with the Department of Electrical Engineering, University of Southern California, Los Angeles, working in optical communications. In 1982, he was Visiting Associate Professor in the Department of Electrical and Computer Engineering, University of Massachusetts, Amherst. From 1976 to 1986, he was a Research Scientist of the Italian National Research Council (CNR) at the Centre di Studio per Metodi e Dispositivi di Radiotrasmissione, Pisa, Italy. From 1986 to 1988, he was Professor of Electrical Engineering at the University of Genoa, Genoa, Italy. From 1988 to 2000, he was Professor of Telecommunications Engineering at the University of Parma, Parma, Italy, where he served as Dean of the Engineering Faculty from 1992 to 1998. He is now Professor of Telecommunications at the Scuola Superiore S.Anna, Pisa, Italy. Since 1995, he is Director of CNIT, Italian Interuniversity Consortium for Telecommunications, incorporating 32 Universities. Since 1997, he has been a Member of the Technical Program Committee of the European Conference on Optical Communications (ECOC). His professional and academic interests are in telecommunication systems and digital signal processing in communications. The activity has focused on optical communications and radiofrequency communications, with application to satellite communications, high-capacity terrestrial digital radio links, mobile radio, modems for switched telephone lines, and fiber communications.